High Pressure Melting Curves of Argon, Krypton, and Xenon:

Deviation from Corresponding States Theory

Reinhard Boehler[1], Marvin Ross[1,2],

Per Söderlind[2] and David B. Boercker[2]

1. Max Planck Institut für Chemie, Postfach 3060, 55020 Mainz, Germany

2. Lawrence Livermore National Laboratory, University of California, Livermore,CA 94551

The melting curves of argon, krypton, and xenon were measured in a laser heated diamond-anvil cell to pressures of nearly 80 GPa reaching melting temperatures around 3300 K. For the three gases we observed a considerable decrease in the melting slopes (dT/dP) from the predictions based on corresponding states scaling starting near 40, 30, and 20 GPa, respectively. The melting anomaly can be understood in terms of a model in which hcp stacking faults act as solutes in a binary system.

High pressure x-ray diffraction studies for solid fcc xenon at room temperature have shown that hcp diffraction lines start to appear over the pressure range from 3.7 to 14 GPa [1-4]. The ratio of hcp/fcc increases continuously with increasing pressure up to about 70-75 GPa

where the conversion to hcp is complete [1, 5]. In the preceding paper Cynn et al.[5] have reported that the martensitic transformation is initially present as stacking disorders in the fcc phase which evolve into the hcp structure at high pressure without evidence for a density discontinuity. At 132 GPa, xenon in the hcp phase becomes metallic[6, 7]. The appearance of an hcp structure and pressure-induced narrowing of the band gap is believed to result from the hybridization of the valence 5p and 5d-like conduction levels [8]. Total energy calculations for krypton and argon predict fcc-hcp transitions at 130 and 220 GPa, respectively, and band gap closure at 310 and 510 GPa [9]. Hcp-like patterns have recently been observed for both gases[5, 10].

Argon melting temperatures have been measured in an externally heated diamond cell to 6 GPa[11], and in a laser-heated diamond cell to 47 GPa[12]. For krypton one melting data point at 23 GPa and 2300 K has been reported[12]. For xenon the only data above 0.7 GPa[13] are two data points near 10 GPa and 2000 K[12]. In this paper we report new measurements of the high pressure melting curves of xenon, krypton and argon to 43, 61 and 77 Gpa, respectively. In all three gases we observed an anomalous lowering in the melting slope that we attribute to the presence of stacking faults.

The melting curves were measured using a diamond cell of our own design. Culet and gasket hole diameters were 0.4 and 0.2 µm, respectively. Schematics of the diamond cell are shown in figure 1. The gasket was made of carbon steel (HRC 60) which was coated with 1 µm diamond powder to increase friction. A disc of tungsten or rhenium with 99.99 % purity and a thickness of about 5 µm that was pressed from an approximately 10 µm grain in a diamond cell was used to absorb the laser light. This disc was thermally insulated from the bottom diamond by either grains of tungsten or rhenium, or a disc of KBr, sapphire or ruby of about 10 µm thickness. Ruby chips for pressure measurement were evenly distributed on the bottom diamond. The gases

were of 99.99 % purity. Argon and Krypton were loaded in the diamond cell at room temperature using a 0.3 GPa gas apparatus. Xenon was loaded at 0 ^{o}C and 55 bar in a gas pressure vessel which was evacuated prior to loading. Without evacuation, lower melting temperatures of xenon were observed, which was most likely due to contamination with air.

Temperatures were generated with an YLF laser (TEM 00, max. power 25 W cw, λ=1.05 µm). At this wavelength only the metal foil in the pressure chamber absorbs the laser radiation. The gas samples itself neither absorbs laser radiation, nor emits incandescent light in detectable amounts. The effective thermal insulation of this tungsten foil from the highly conductive diamonds by both the KBr disc on one side and the gas pressure medium (and sample) on the other side allows a defocused laser beam and, thus, minimizing radial temperature gradients. The onset of melting (see below) can then be observed from a large, uniformly heated area of at least 20 µm in diameter in the center of the hot spot. Temperature profiles for a nearly identical sample geometry have been documented elsewhere[14, 15]. The temperature gradients in the axial direction away from the tungsten foil do not effect melting (or freezing) experiments, because the sample in direct contact with the metal foil has the same temperature as the metal surface from which the temperature is measured. We collected the incandescent light from areas of 1-2 µm diameter in the wavelength range 550–800 nm with a CCD (charge-coupled-device) detector, and the temperature was determined by fitting a Planck radiation function to the emission spectra with both temperature and emissivity as free parameters. Temperature can be measured in this way with a precision of ±10 K, but at the highest temperatures measured here there is an uncertainty of order 100 K due to the unknown emissivity-wavelength dependence of tungsten at high pressure. Measurements below 1500 K become unreliable due low light intensity

.

Melting was detected with the laser speckle method described previously[16]: The blue light (488 nm, 5 mW, cw) of an argon laser created an interference pattern on the surface of the

metal foil. When this surface reached the melting temperature of the sample, motion in this pattern was observed. This motion is due to local changes in the refractive index in the thin liquid, convecting xenon layer in contact with the metal foil. This method for measuring melting temperatures has been extensively tested for noble gases[2, 12] and for the alkali halides[16] where the results can be directly compared with low pressure melting data obtained using thermocouples. Temperatures were measured at the onset of this motion when the temperature was slowly increased or at the disappearance of motion at decreasing temperature. The measured melting and freezing temperatures were within the experimental uncertainty which was estimated from a minimum of five melting-freezing cycles to be ±100 K. The surface of the metal discs did not show any sign of chemical reaction.

Plotted in figure 2 are our measurements of the melting data for Xe, krypton, and argon. These results are in very good agreement with those reported by Jephcoat and Besedin[12]**.** Up to about 20, 30, and 40 GPa, the measurements for Xe, Kr, and Ar, are in good agreement with predictions from corresponding states scaling from the neon melting curve [17]. Above these pressures there occurs a significant lowering of the melting temperatures from corresponding states. Since the fcc-hcp and metallization transitions of the heavy rare gases are best understood for xenon, we focus the remainder of our discussion on this gas.

The possibility that thermal electron excitation is responsible for the change in melting slope was considered. However, at this pressure the measured optical band gap in the solid, E_g, is about 6 eV[18, 19], and since the ratio $E_g/kT=25.8$ is rather large, such an effect may be considered negligible**.** If electronic excitation occurred only in the liquid then a change on coloration would appear upon melting which would increase in intensity with increasing pressure. This is not observed. Also, shockwave studies show that significant thermal excitation in liquid xenon and argon begins at about 10,000 K and 12,000 K, respectively[20, 21].

A discontinuous change in the melt slope is usually indicative of a solid-solid phase transition. At such a transition the density of the solid increases abruptly in contrast to that of the liquid, and the melting slope turns up. However, the present case is quite unusual in that the melting slope decreases. In the case of xenon, the slope predicted by corresponding states melting above 20 GPa is dT/dP~56 K/GPa while the slope observed is only 24 K/GPa. Such a large decrease in the slope infers either that at the transition the liquid density increases or the density of the new solid phase decreases. It is difficult to find a reasonable mechanism in favor of either of these two possibilities. Since the unexpected decrease we observe in the melting slope occurs over roughly the same pressure range as the appearance of significant fractions of stacking faults it is reasonable to assume that the two phenomena are closely related. The higher pressure for the start of the anomaly along the melting curve, than along the room temperature isotherm, is consistent with observations by Yoo (personal communication) that the pressure at which stacking faults first appear increases with increasing temperature.

It is known that the addition of impurity atoms into a crystal to form a disordered alloy leads to a decrease in the melting temperature with respect to the pure crystal. [22, 23]. We therefore suggest that hcp microstructures behave as impurities in fcc-xenon leading to a lowering of melting temperatures. The expression for the melting curve of the defective crystal in equilibrium with the pure liquid becomes,

$$T_d = T_o(1-x). \qquad \text{Eq. 1}$$

Where T_o is the temperature along the corresponding states melt line. Since Cynn et al. have observed that the ratio of hcp increases linearly with pressure we assume that the mole fraction, x, of hcp-like defects increases linearly with increasing pressure starting from 22 GPa, the pressure at which the experimental and corresponding states melt curves cross.

It is apparent that with increasing pressure the xenon melting curve must rise and eventually converge with the corresponding states curve of the pure hcp phase near 75 GPa. In approaching this higher pressure hcp limit the defect solute particles will have the fcc structure. To accommodate both limits in a single expression we rewrite Eq. 1 as;

$$T_d = T_o\{1-x(1-x)\} \qquad \text{Eq. 2}$$

The expression for mole fraction is: $x = (P - P_L)/(P_U - P_L)$, where P is the pressure and P_L and P_U are 22 and 75 GPa, respectively.

The calculated melting temperatures from this approximate model, shown in Fig. 3, are in good agreement with experiment. The model predicts an increase in the melting slope above 40 GPa. Similar results have been obtained in the case of melting temperatures at atmospheric pressure for alkali metal mixtures of varying concentrations[24]. In contrast to these studies, the impurity concentration in the present work is pressure-induced.

The difference between the solidus and the liquidus temperature in a binary system cannot be measured in our experimental set-up due to the temperature gradient in the optical axis. However, the temperature measured at the onset of melting is most likely reasonably close to the eutectic temperature, as has been shown for the eutectic Fe-S system[25].

Stacking faults may be understood by considering the polytypism of close-packed structures where the layers of atoms can be labeled "A","B" or "C". Stacking these layers in the sequence ABCABC leads to an fcc lattice and hcp has the sequence ABABAB. There are an infinite number of such close-packed structures between fcc and hcp. For example, ABAC is dhcp and ABACACBCB is the Sm-type. However, as noted by Kittel[26], there may exist structures in which the stacking sequence is not periodic. For example, a stacking fault may be formed in an fcc lattice by moving A planes to B positions, and B planes to C positions, so that

ABCABCAB… becomes ABCBCABC..., and so on. Thus, stacking faults in an fcc lattice may locally create hcp structures, ABCABAB. The presence of stacking faults are closely related to crystal stability.

Total energy calculations were made for several close-packed structures of xenon: fcc, dhcp, hcp and bcc phases at 0 K using the full-potential linear muffin-tin orbital (FP-LMTO) method[27]. The results are plotted versus pressure in Fig. 4 as the energy differences, where hcp=0 is the reference energy. Up to 50 GPa the energies of fcc and hcp (also the dhcp and Sm structures not shown) are within numerical accuracy (±1 mRy/atom). bcc is the least stable over the pressure range. The calculations predict that hcp and fcc have nearly the same energy at ambient pressure and the hcp structure becomes increasingly stable relative to fcc. However, we know that the fcc phase is the more stable at ambient conditions and that hcp becomes more stable phase above 75 GPa. Therefore, we have lowered the fcc energy by 1 mRy, creating curve fcc-1 in Fig. 2, which crosses above the hcp curve at 75 GPa. This new curve shows more clearly the decrease in energy separating the fcc and hcp phases occurring with increasing pressure. Since the energy separating the fcc and hcp lattices is small, it is reasonable to expect that, thermal fluctuations will occasionally slide the position of an fcc plane to an hcp arrangement leading to an hcp stacking fault. The fact that DAC studies[5] show the fraction of hcp increases with increasing pressure is consistent with this picture.

Stacking faults are essentially defects which act to raise the free energy with respect to a perfect crystal and lower the melting temperature. Since the number of stacking faults increases with increasing pressure this leads to a lowering of the melting slope, as shown in Fig. 3, and an expected reversal when fcc faults become the defect in the hcp lattice.

References

[1] A. P. Jephcoat, *et al.*, Phys. Rev. Lett. **59**, 2670 (1987).

[2] A. P. Jephcoat, *et al.*, in *AIRAPT*, Kyoto, Japan, 1997).

[3] W. A. Caldwell, *et al.*, Science **277**, 930 (1997).

[4] C.-S. Yoo, *personal communication*

[5] H. Cynn, *et al.*, Phys. Rev. Lett. this issue.

[6] K. A. Goettel, *et al.*, Phys. Rev. Lett. **62**, 665 (1989).

[7] R. Reichlin, *et al.*, Phys. Rev. Lett. **62**, 669 (1989).

[8] A. K. McMahan, Phys. Rev. B **33**, 5344 (1986).

[9] I. Kwon, *et al.*, Phys. Rev. B **52**, 15165 (1995).

[10] L. S. Dubrovinsky, *pers. communication*

[11] C.-S. Zha, *et al.*, J. Chem. Phys. **85**, 1034 (1986).

[12] A. P. Jephcoat and S. Besedin, in *US-Japan Conference in Mineral Physics*, edited by M. Manghnani and T. Yagi (AGU Publications, Washington,DC, 1997).

[13] P. H. Lahr and W. G. Eversole, J. Chem. Eng. Data **7**, 42 (1962).

[14] R. Boehler, N. V. Bargen, and a. Chopelas, J.Geophys. Res. **95**, 21731 (1990).

[15] R. Boehler, Rev. Geophys. **38**, 221 (2000).

[16] R. Boehler, M. Ross, and D. B. Boercker, Phys. Rev. Lett. **78**, 4589 (1997).

[17] W. L. Vos, *et al.*, J. Chem. Phys. **94**, 3835 (1991).

[18] K. Syassen, Phys. Rev. B **25**, 6548 (1982).

[19] K. Asaumi, Phys. Rev. B **29**, 7026 (1984).

[20] M. Ross and A. K. McMahon, Phys. Rev. B **21**, 1658 (1980).

[21] M. Ross, *et al*., J. Chem. Phys. **85**, 1028 (1986).

[22] P. R. Okamoto, N. Q. Lam, and L. E. Rehn, in *Solid State Physics*, edited by H. Ehrenreich and F. Spaepen (Academic Press, New York, 1999), Vol. 52, p. 1-133.

[23] P. C. Liu, *et al*., Phys. Rev. B **60**, 800 (1999).

[24] S. Rabinovich, A. Voronel, and L. Peretzman, J. Phys. C: Solid State Phys. **21**, 5943 (1988).

[25] R. Boehler, Phys. Earth Planet. Int. **96**, 181-186 (1996).

[26] C. A. Kittel, *Introduction to Solid State Physics* (John Wiley & Sons, New York, 1996).

[27] P. Soderlind, J. A. Moriarty, and J. M. Wills, Phys. Rev. B **53**, 14063 (1996).

Figure captions

Fig. 1 Schematic description of the diamond-anvil-cell for high temperature melting studies.

Fig. 2 Melting curves of xenon (A), krypton (B), and argon (C). Closed circles are the present melting measurements and the open circles are those of Jephcoat and Besedin[12]. At the highest pressures the uncertainty in the melting temperature of xenon is about ±100 K. Argon measurements below 7 GPa are from Zha et al[11].The dashed lines are the predicted melting curves obtained by corresponding states scaling from the neon melting curve [17].

Figure 3. Open circles are the present xenon melting measurements. The solid line, is the predicted xenon melting curve obtained by corresponding states scaling from the argon measurements. The dashed line was calculated using the alloy model of Eq. 3, as discussed in text.

Figure 4. Energy differences of xenon for fcc, hcp, bcc, and fcc-1 are plotted as a function of pressure (hcp, the dashed line, is the reference energy).

Figure 1

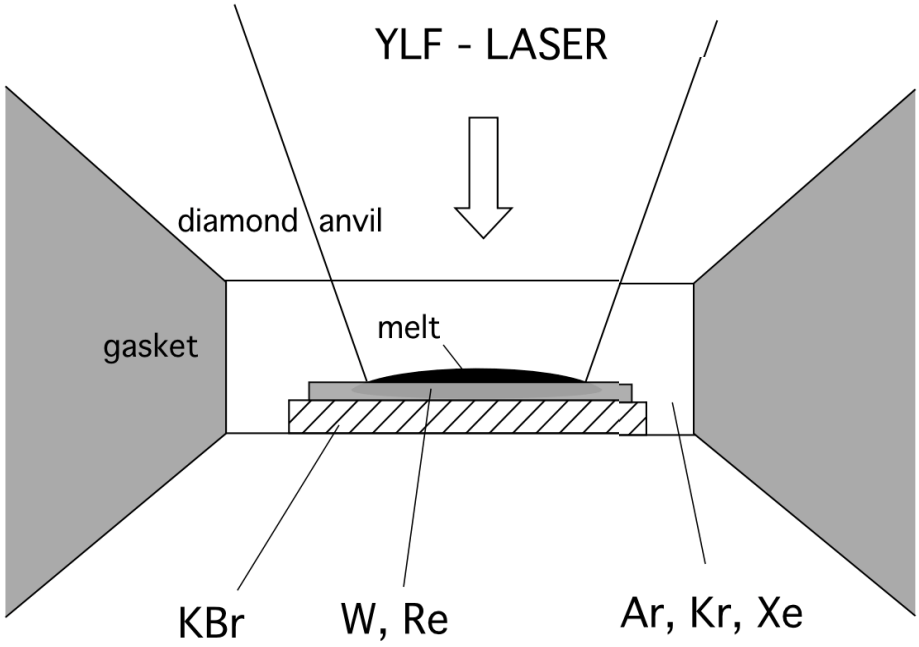

Figure 2 A

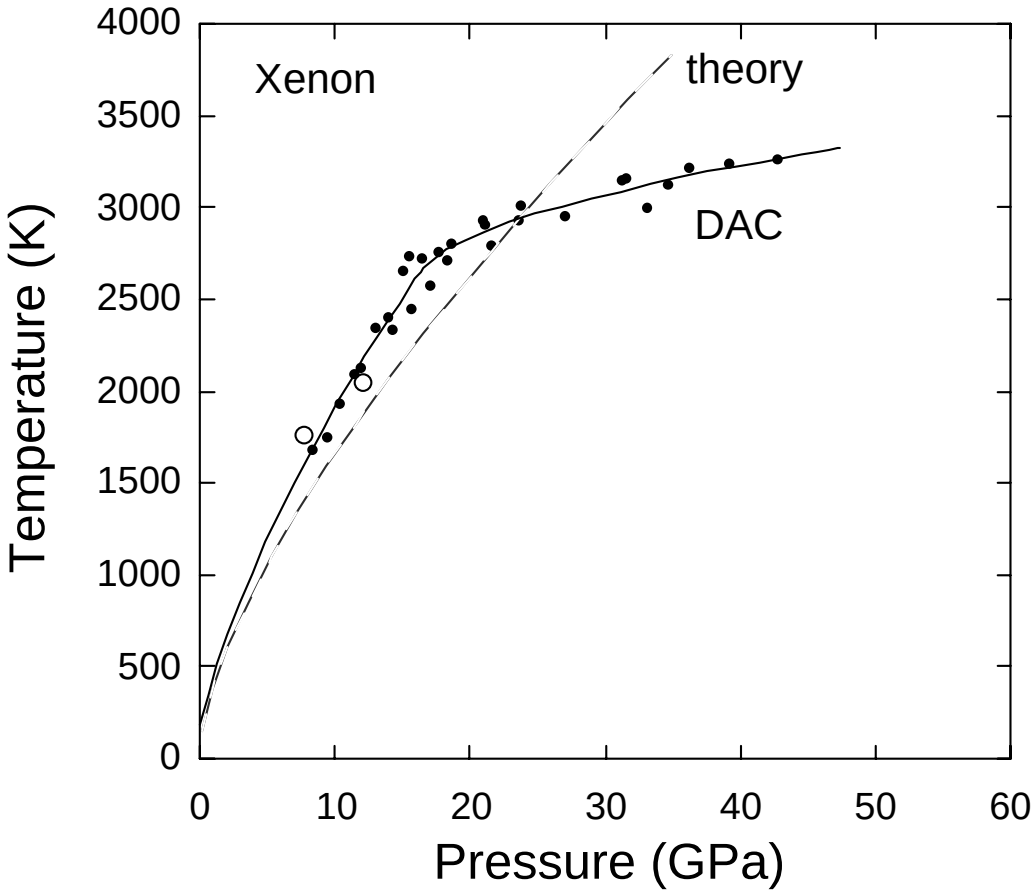
Xenon
theory
DAC
Temperature (K)
Pressure (GPa)
0
500
1000
1500
2000
2500
3000
3500
4000
0
10
20
30
40
50
60

Figure 2 B

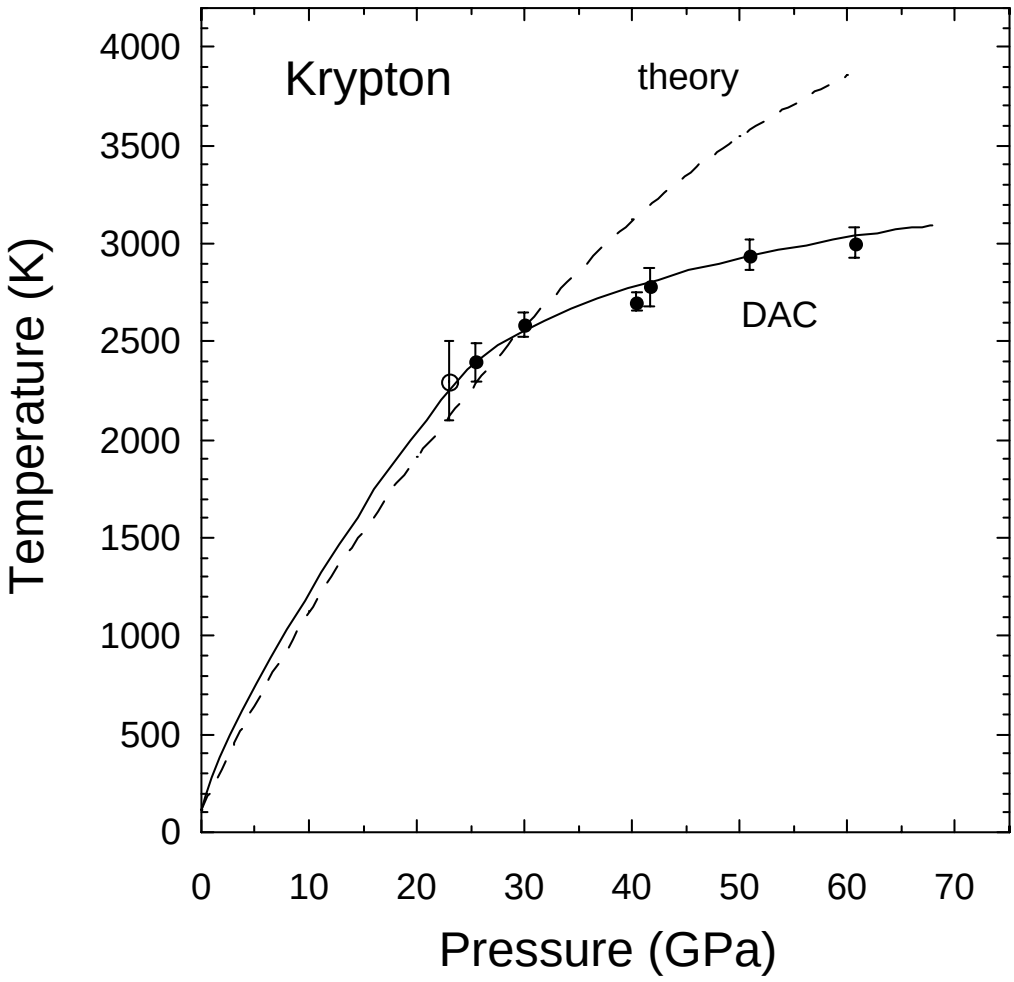
Krypton
theory
DAC
Temperature (K)
Pressure (GPa)
0
500
1000
1500
2000
2500
3000
3500
4000
0
10
20
30
40
50
60
70

Figure 2 C

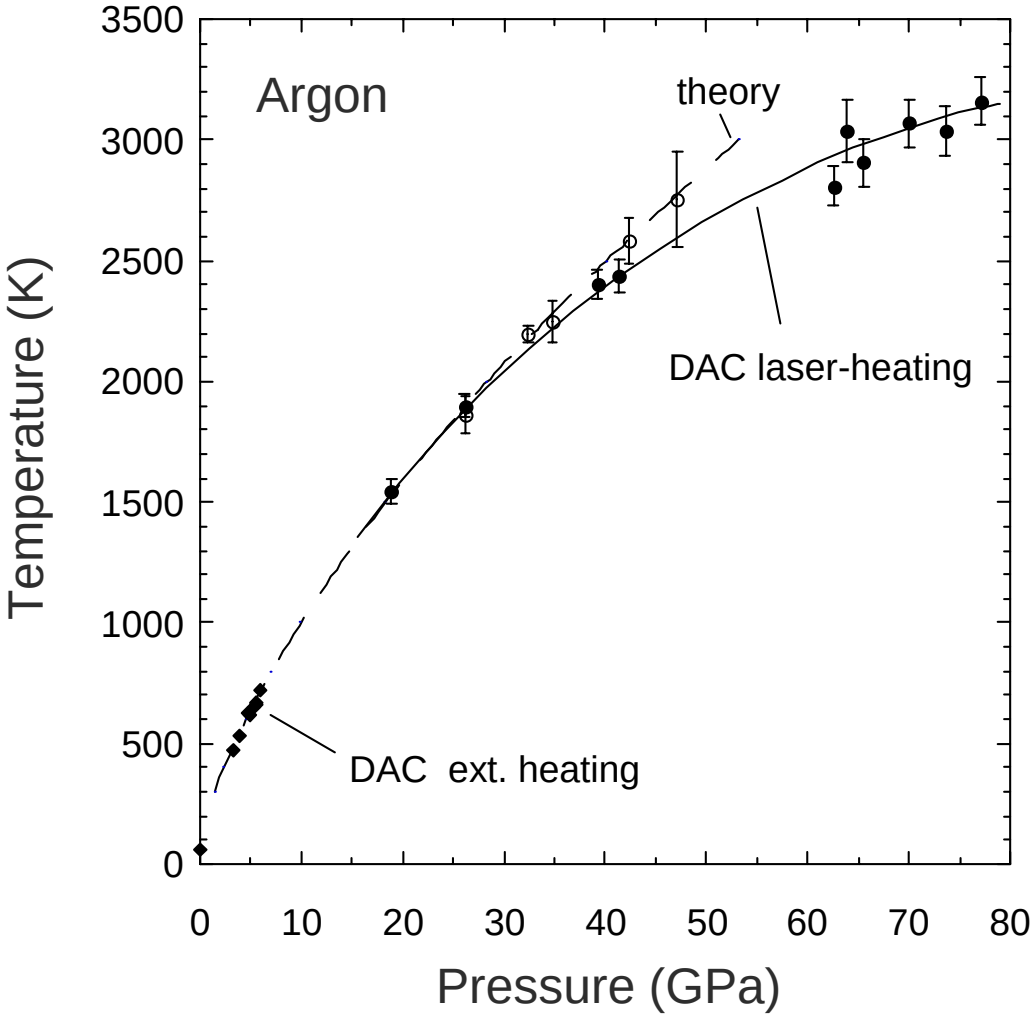
Argon
theory
DAC laser-heating
DAC ext. heating
Temperature (K)
Pressure (GPa)
0
500
1000
1500
2000
2500
3000
3500
0
10
20
30
40
50
60
70
80

Figure 3

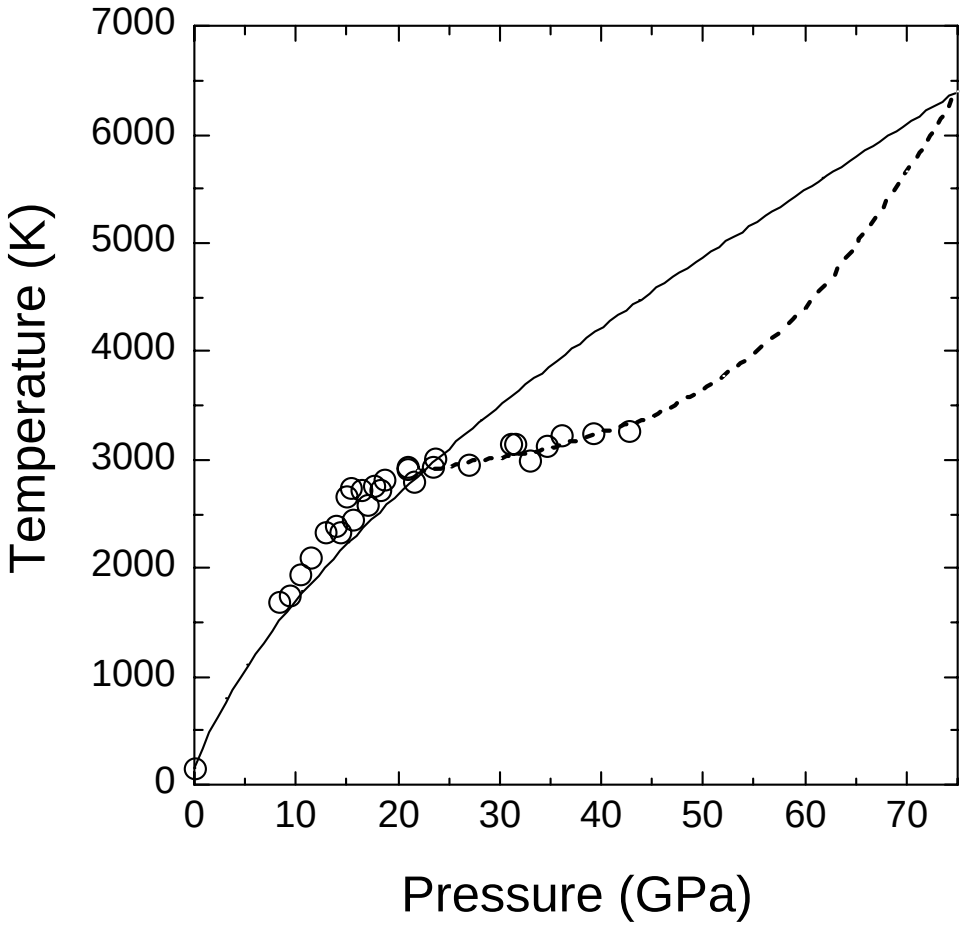
Temperature (K)
Pressure (GPa)
0
1000
2000
3000
4000
5000
6000
7000
0
10
20
30
40
50
60
70

Figure 4

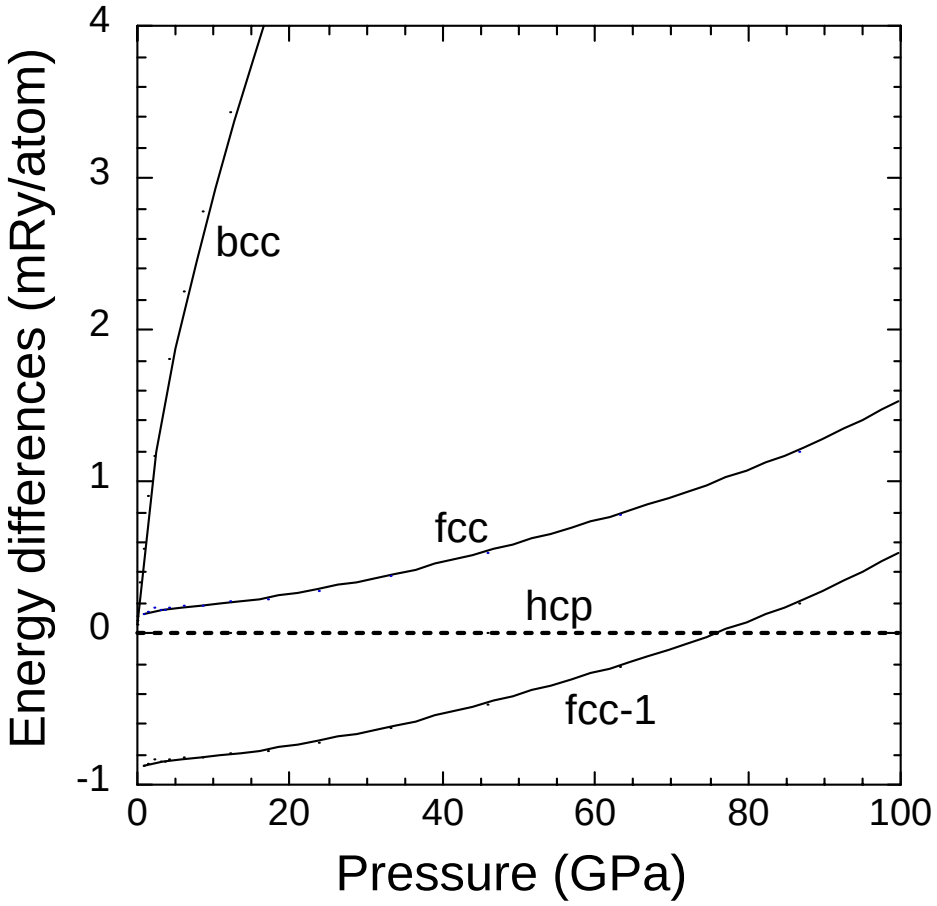
Energy differences (mRy/atom)
Pressure (GPa)
bcc
fcc
hcp
fcc-1
4
3
2
1
0
-1
0
20
40
60
80
100